NASA CR-120874

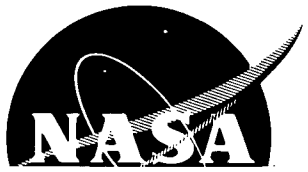

(NASA-CR-120874) IMPROVEMENT OF A LARGE-AMPLITUDE SINUSOIDAL PRESSURE GENERATOR FOR DYNAMIC CALIBRATION OF PRESSURE R.E. Robinson (Battelle Memorial Inst.) Feb. 1972 31 p CSCL 14B G3/14

N72-21428

Unclas 24418

IMPROVEMENT OF A LARGE-AMPLITUDE SINUSOIDAL PRESSURE GENERATOR FOR DYNAMIC CALIBRATION OF PRESSURE TRANSDUCERS

by

Richard E. Robinson

Prepared for

NATIONAL AERONAUTICS AND SPACE ADMINISTRATION

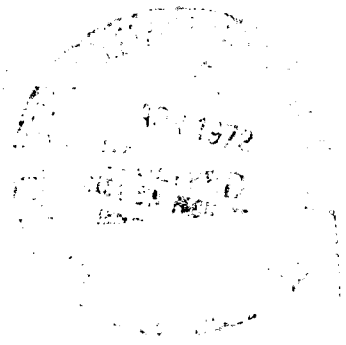

NASA Lewis Research Center
Contract NAS 3-11229
Richard J. Priem, Project Manager
Chemical Propulsion Division
Marshall C. Burrows, Technical Monitor
Physics and Chemistry Division

BATTELLE
Columbus Laboratories
505 King Avenue
Columbus, Ohio 43201

25

1. Report No.	2. Government Accession No.	3. Recipient's Catalog No.
NASA CR-120874		

4. Title and Subtitle	5. Report Date
IMPROVEMENT OF A LARGE-AMPLITUDE SINUSOIDAL PRESSURE GENERATOR FOR DYNAMIC CALIBRATION OF PRESSURE TRANSDUCERS	February 1972
	6. Performing Organization Code
7. Author(s)	8. Performing Organization Report No.
Richard E. Robinson	
	10. Work Unit No.
9. Performing Organization Name and Address	11. Contract or Grant No.
Battelle Columbus Laboratories 505 King Avenue Columbus, Ohio 43201	NAS 3-11229
	13. Type of Report and Period Covered
12. Sponsoring Agency Name and Address	Contractor Report
National Aeronautics and Space Administration Washington, D.C. 20546	14. Sponsoring Agency Code

15. Supplementary Notes

Project Manager, Richard J. Priem, Chemical Propulsion Division, NASA Lewis Research Center, Cleveland, Ohio, and Technical Monitor, Marshall C. Burrows, Physics and Chemistry Division, NASA Lewis Research Center, Cleveland, Ohio

16. Abstract

Results of research on the improvement of a sinusoidal pressure generator are presented. The generator is an inlet-area-modulated, gas-flow-through device (siren type) which has been developed to dynamically calibrate pressure transducers and pressure probes. Tests were performed over a frequency range of 100 Hz to 20 kHz at average chamber pressures (bias pressure) between 30 and 50 psia (21 and 35 N/cm^2abs) and between 150 and 300 psia (104 and 207 N/cm^2abs). Significant improvements in oscillation pressure waveform were obtained but with reduction in available generator oscillation pressure amplitude range. Oscillation pressure amplitude, waveform, and waveform spectral content are given as functions of frequency for the two bias pressure conditions. The generator and instrumentation for frequency, amplitude, and spectrum measurements are described.

17. Key Words (Suggested by Author(s))	18. Distribution Statement
Pressure measurements Transducer testing Frequency response Pressure generator Pressure oscillation	Unclassified - unlimited

19. Security Classif. (of this report)	20. Security Classif. (of this page)	21. No. of Pages	22. Price*
Unclassified	Unclassified	22	

*For sale by the National Technical Information Service, Springfield, Virginia 22151

FOREWORD

This report summarizes the efforts performed by Battelle's Columbus Laboratories under NASA Contract No. NAS 3-11229 from December 15, 1970, through June 15, 1971. The project manager was Dr. Richard J. Priem, Chemical Propulsion Division, and the technical monitor was Dr. Marshall C. Burrows, Physics and Chemistry Division, National Aeronautics and Space Administration, Lewis Research Center, Cleveland, Ohio 44135.

The author wishes to acknowledge the contribution of several individuals to the work described in the report. Dr. C. Y. Liu advised throughout the program, Mr. R. E. Hess participated in data analyses, and R. J. McAninch assisted in the performance of tests. Special acknowledgement is also given to Mr. Sanford Meiselman, representative for the Pall Corporation, who provided many test material samples without charge.

IMPROVEMENT OF A LARGE-AMPLITUDE SINUSOIDAL PRESSURE GENERATOR FOR DYNAMIC CALIBRATION OF PRESSURE TRANSDUCERS

by

Richard E. Robinson

SUMMARY

Results of research on the improvement of a sinusoidal pressure generator are presented. The generator is an inlet-area-modulated, gas-flow-through device (siren type) which has been developed to dynamically calibrate pressure transducers and pressure probes. Oscillation pressure waveform was improved by the addition of several porous inserts to the generator test chamber. Three of the six generator operating modes were tested which included determining upper and lower oscillation pressure amplitude bounds. Tests were performed over a frequency range of 100 Hz to 20 kHz at average chamber pressures (bias pressures) between 30 and 50 psia (21 and 35 N/cm^2abs) and between 150 and 300 psia (104 and 207 N/cm^2abs) using the nominal generator operating mode. Peak-to-peak oscillation pressure amplitudes of 153, 73, 11, and 7 percent of bias pressure were obtained at frequencies of 100, 1,000, 10,000, and 20,000 Hz, respectively. Best oscillation pressure waveform was obtained between fundamental frequencies of 1 kHz and 5 kHz were second, third, and fourth harmonic frequency amplitudes were 7, 3.5, and 2 percent of the fundamental frequency amplitude. Peak-to-peak oscillation pressure amplitudes could be increased or reduced by using additional constant-flow inlets and outlets. Without the porous inserts in the generator chamber, peak-to-peak oscillation pressure amplitudes approximately doubled.

The generator and instrumentation for making frequency, amplitude, and pressure measurements are described.

INTRODUCTION

The need to measure "nonsteady" pressure has existed for many years and recent developments have increased the requirements and complexities of these measurements. Large "nonsteady" pressure amplitudes over wide ranges of bias pressure and frequency are being encountered. In addition, protection from severe environments and space limitations have added further complexities requiring new small, high-frequency transducers in devices such as probes and cavities with coolant bleeds and coatings. Accompanying these measurement needs is the need for dynamic calibration of the pressure transducers and their interfacing connections at the new pressure and frequency conditions.

The dynamic performance characteristics of pressure transducers and pressure-measuring systems can be determined directly by a sinusoidal pressure generator. Battelle-Columbus studied methods for generating large-amplitude, high-frequency pressure fluctuations.[1]* The result of the methods study was that an inlet-area-modulated, gas-flow-through device (siren type) showed the most potential for advancing the state of the art.

Effort was undertaken to design, construct, and evaluate an inlet-modulated sinusoidal pressure generator (IM-SPG).[2] The major results of the development and evaluation tests performed following the design and construction of the IM-SPG were:[2]

- The specified ratios of peak-to-peak oscillation pressure amplitude to average pressure of 1.0 at 15 Hz and 0.12 at 10,000 Hz were obtained.

- The waveform of the transducer output signal consisted primarily of the driving (fundamental) frequency sinusoid but also contained considerable higher harmonic and transducer resonant frequency band components. This waveform distortion would limit the IM-SPG in its present form as a dynamic pressure-transducer calibrator to low frequencies (several thousand Hz) or for less stringent evaluation tests of pressure measuring systems up to 15,000 Hz.

Following this, the present study was undertaken to gain a more complete understanding of the performance of the IM-SPG and to improve its oscillation pressure waveform.

This report summarizes the waveform-improvement development program and presents the IM-SPG performance (amplitude and waveform) obtained. The generator was then utilized by investigating the dynamic response characteristics of six frequently used, current, high-frequency pressure transducers. Amplitude ratios as functions of frequency and bias pressure were determined and are reported in a companion report.[3]

TEST APPARATUS AND PROCEDURE

Generator

The design concept of the sinusoidal pressure generator, an inlet-modulated, gas-flow-through device, is shown in Figure 1. Pressure oscillations in this type of generator are produced by changing the mass content in a chamber by controlling the gas flow into and out of the chamber. The oscillating or sinusoidally varying static pressure in the chamber is used to

* Numbers in parentheses refer to references listed at the end of this report.

dynamically calibrate pressure transducers. The pressure in the chambers is sensed by the flush-mounted test transducer and by a flush-mounted reference or standard transducer.

Basically, the generator consists of a cylindrical chamber with a modulated inlet flow opening and a fixed outlet flow opening (See Figure 1.). The chamber is 0.75 inch (1.91 cm) in diameter and 0.262 inch (0.665 cm) in length. A result of this program is that, for improved waveform, the chamber is filled with two types of porous materials (acoustic absorbing filler). This filler improves pressure wave shape by reducing chamber harmonics and flow turbulence (which excites transducer resonances). The two flow openings are placed on the curved cylinder sides (diametrically opposite each other). One of the flat end surfaces of the cylinder is used for flush mounting the test transducer or measuring system under evaluation. The reference transducer is flush mounted on the opposite flat cylinder end. Two additional openings through the cylindrical wall are provided. They can serve independently, in any combination as either inlets or outlets, or be plugged. The various combinations of openings (generator operating modes) offer additional control of average chamber (bias) pressure independent of pressure fluctuation amplitude.

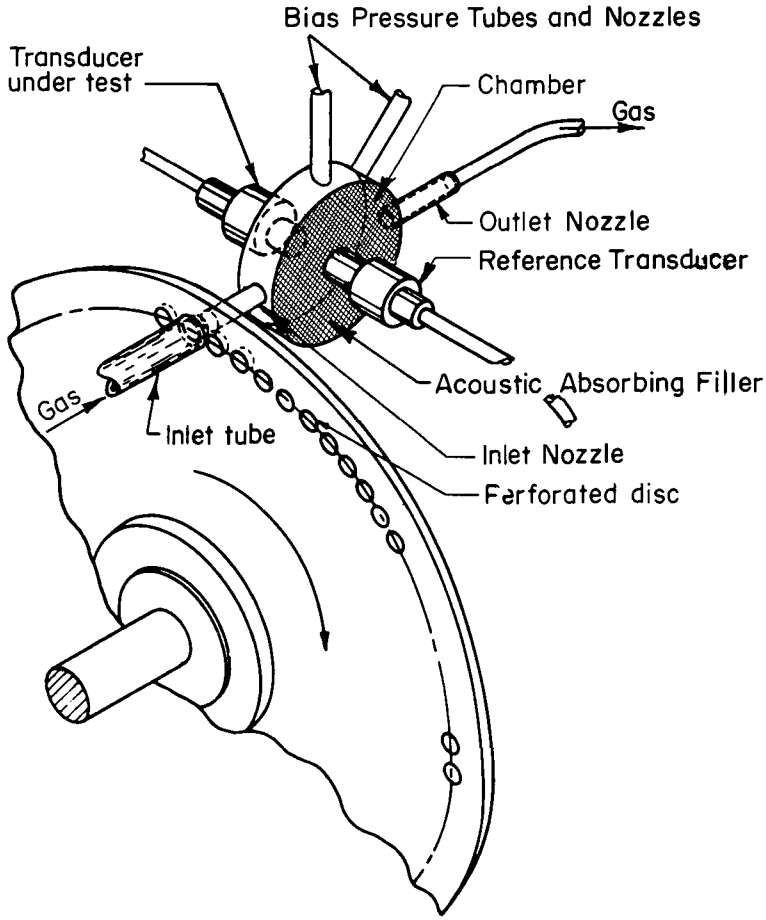

FIGURE I. INLET-MODULATED SINUSOIDAL PRESSURE GENERATOR

Inlet opening area modulation is achieved by rotating a circular disc with numerous holes located along a circle near the disc periphery against the inlet nozzle throat. The disc holes are the same size and shape as the nozzle throat. They are equally spaced two hole diameters apart around the hole-circle. All flow openings are operated at supercritical flow conditions. A more detailed description of the generator is given in Reference 2.

Instrumentation

Instrumentation was set up in conjunction with the pressure generator to measure frequency, oscillation pressure amplitude, and waveform spectrum of the reference transducer along with chamber pressure. A schematic of the measuring-system layout is shown in Figure 2. Frequency is measured with an electronic counter and a magnetic pickup which senses or counts the holes in the generator rotating disc. For pressure-amplitude measurements, the conditioned signal from a charge amplifier is normally split. One signal is displayed on one channel of a high frequency dual beam oscilloscope. The other signal, low-pass filtered at 50 kHz, is displayed on the other channel of the oscilloscope. The oscilloscope is externally triggered by a manually operated switch in a trigger line between the IM-SPG and the oscilloscope. Another magnetic pickup provides the trigger signal by sensing a single notch on the outer periphery of the rotating chopping disc. Thus, the same holes were utilized and provided repeated area modulation and the resultant pressure oscillations in each test. The waveforms displayed on the oscilloscope were photographed. The 50-kHz low-pass filter was used to smooth out any small suppressed transducer ringing remaining in the signal and thus achieve data-reduction accuracy. A single-channel spectrum analyzer (storage oscilloscope plug-in unit) was used to measure waveform spectral content of either the filtered or unfiltered signal. The unfiltered pressure amplitude signal of the reference transducer was also measured by a high-frequency true-root-mean-square meter and manually recorded. This latter measurement provided a quick check on pressure-amplitude consistency. Average chamber pressure was measured by a pressure transducer connected to the generator chamber by 3 feet (0.91 m) of 1/8-inch-(0.32 cm)-diameter tubing. The tubing was flush mounted in the chamber (in place of the test transducer) using a replacement adaptor for the test transducer adaptor.

In addition to static electrical calibrations, all instruments and the integrated systems were calibrated for frequency response using a high-frequency electronic signal generator. It was found that the output of the charge amplifiers used for conditioning the piezoelectric pressure transducer signals had to be corrected in amplitude at high frequencies and high amplification levels. The low-pass filter and charge amplifier frequency-response characteristics are given in the Appendix to this report.

Procedure

The present effort was directed at improving the pressure waveform. Consequently, the final evaluation tests reported in Reference 2 were modified to provide preliminary information to guide the waveform-improvement work. A

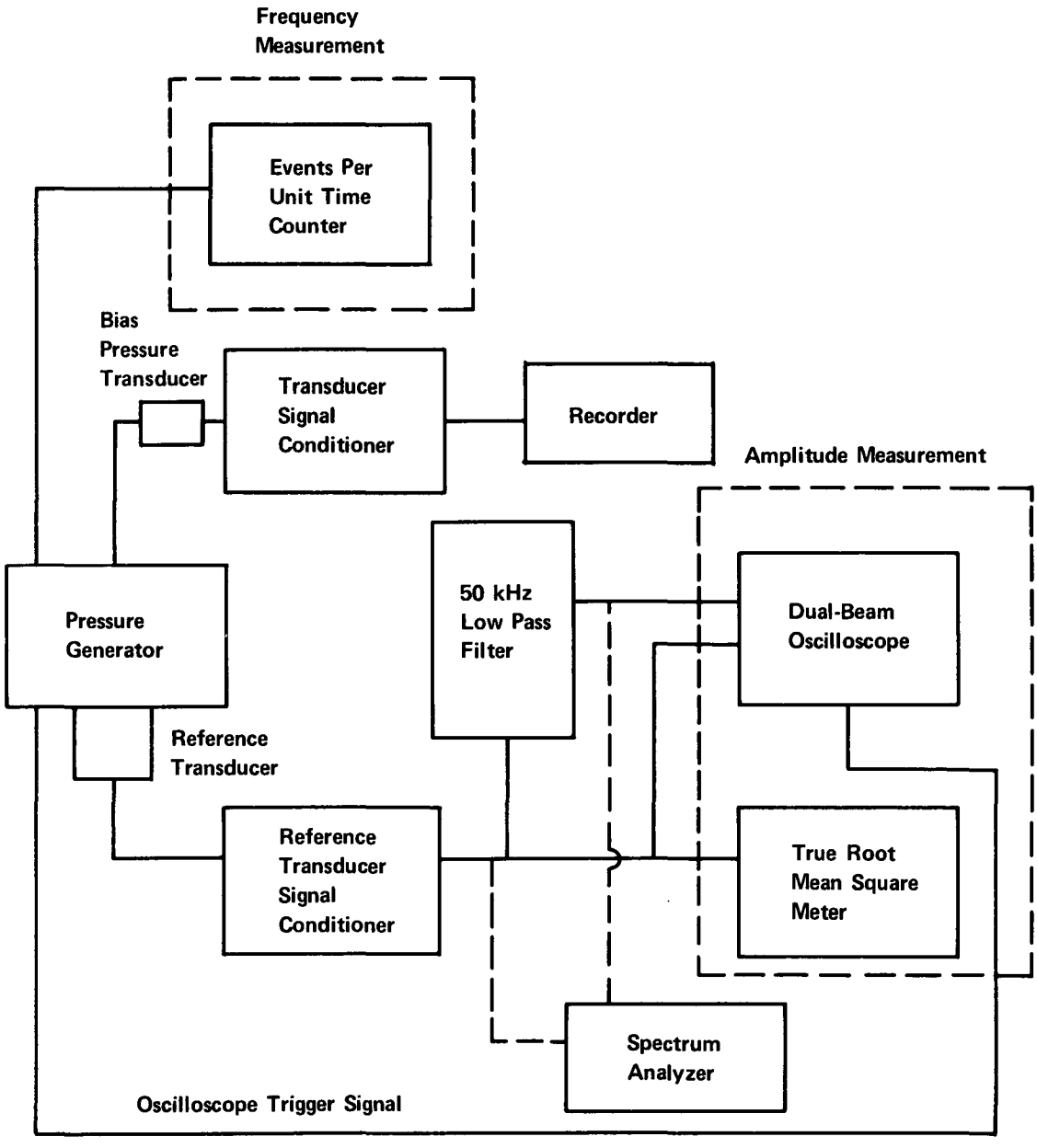

FIGURE 2. TEST APPARATUS LAYOUT

series of IM-SPG tests was made to analyze the reference transducers output signal. Tests were made with different electronic filtering conditions varying from 1.3 to 25 times the waveform fundamental (or SPG driving) frequency. These tests helped to determine the frequency content of the signal. Several different filters were used to determine if the various electronic circuits were interacting and affecting the signal displayed on the oscilloscope. No interaction was found.

Next a series of tests was performed in which a spectrum analyzer was added to obtain oscillation pressure waveform and waveform frequency content. Tests were run at different frequencies (1 kHz, 3 kHz, 5 kHz, and 10 kHz) at low pressure [chamber pressure = 50 psia (35 N/cm^2abs)]. Several more empty-chamber tests were performed at high chamber pressures [150 to 300 psia (104 to 207 N/cm^2abs)].

Typical oscillation pressure waveform spectral content is given in Table 1.

TABLE 1. WAVEFORM SPECTRAL CONTENT AMPLITUDE IM-SPG WITHOUT ACOUSTIC FILLER

Fundamental Frequency, kHz	Harmonic Amplitude - Percent Fundamental for Indicated Harmonic			
	2	3	4	5
1	5	<1	<1	<1
3	8	6	4	<1
5	18	11	6	<1
10	50	28	27	20

A filtered and unfiltered oscillation pressure waveform and the spectral content of the unfiltered signal are shown in Figure 3.

The approach selected to reduce the high-frequency components was to use flow-smoothing devices such as screens or porous materials downstream of the chamber inlet nozzle. The inlet-nozzle flow is quite complex. A simple conical-divergent section is designed to operate as overexpanded throughout the pressure oscillation at all useable frequencies. Thus, the flow in the nozzle is shocked from supersonic to subsonic within the nozzle. This most likely occurs through an oblique shock structure rather than a normal one and can introduce large-amplitude pressure waves with attendant high-frequency components that excite the pressure transducer at or near its resonant frequency.

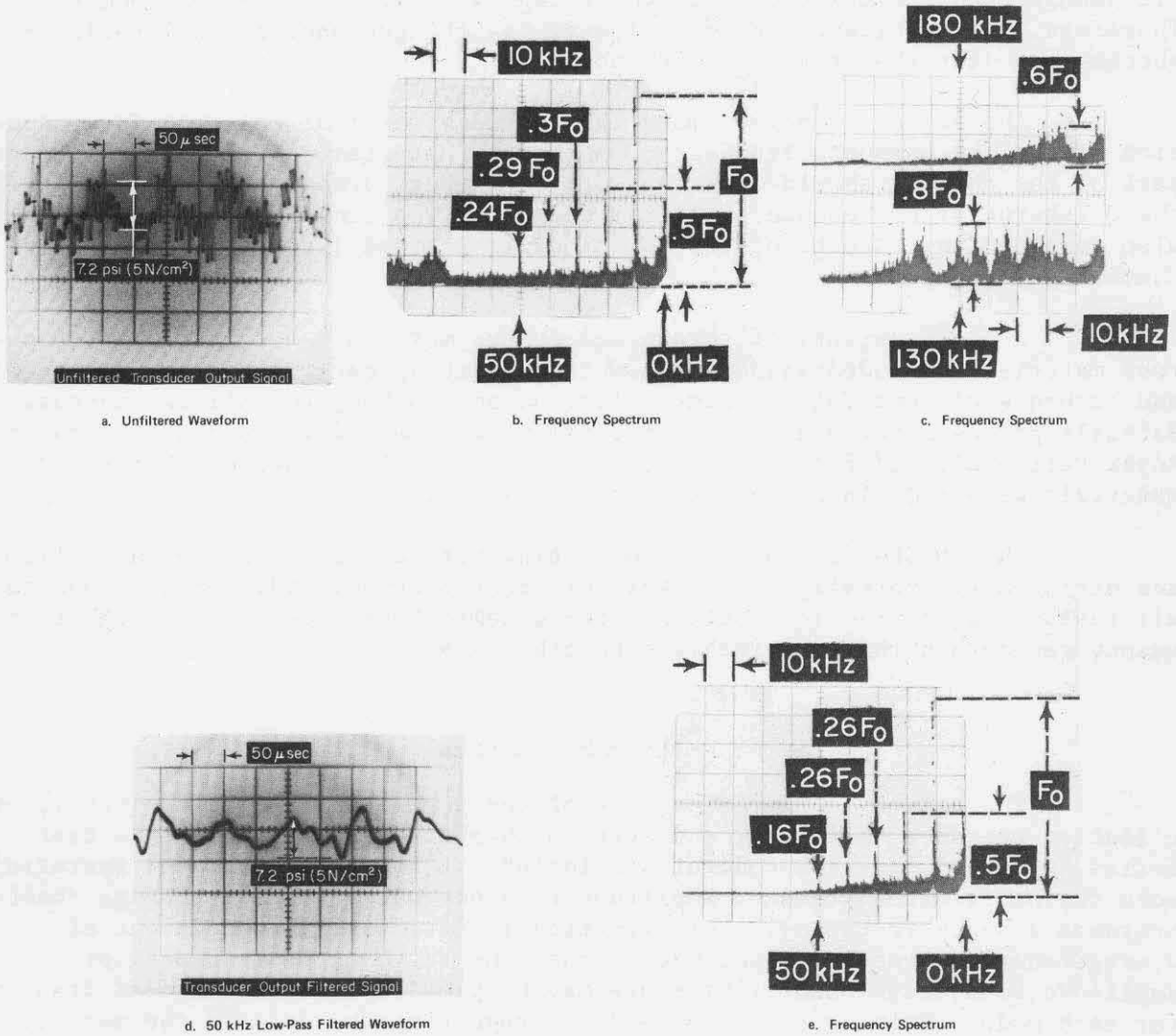

a. Unfiltered Waveform

b. Frequency Spectrum

c. Frequency Spectrum

d. 50 kHz Low-Pass Filtered Waveform

e. Frequency Spectrum

Figure 3. Pressure waveform and frequency spectrum from oscilloscope. Frequency, 10 kHz; bias pressure, 50 psia (35 N/cm^2-abs); IM-SPG test chamber without acoustic filler; IM-SPG operating mode, one inlet/one outlet.

Note: Amplitude called out includes filter and charge amplifier correction.

The inlet-nozzle flow is further complicated by the area modulation of its throat. Besides the changes in area and size required to produce the pressure oscillation, the throat shape and its location relative to the down stream expansion section change throughout a cycle. These conditions are depicted in Figure 4. It can be seen that a flow jet through an essentially crescent-shaped area at the side of the divergent section exists during a cycle. This jet may be at an angle to the chamber dependent upon wheel clearance. The conical-divergent section cross-sectional geometry corresponds in shape to the throat shape for symmetrical flow only once in the cycle--it does not change shape to coincide with the changing cyclic throat-area geometry. Therefore, the resultant flow most likely has oblique shocks, wall-reflected shocks, and jets that enter the SPG chamber.

The screen or porous-material approach was also selected for reduction of the low harmonic frequency component. Material addition in the central part of the chamber should damp the normal chamber harmonics--that is increase the Q (sharpness of resonance) of the chamber. The central chamber material also dampened any effects of the inlet nozzle jet and jet reflections from chamber walls.

A large variety of screen and porous materials was tested. The porous materials included standard acoustic absorbing materials, sponges, steel and carbon wools and felts, foamed aluminum and carbon, and silica, inhouse Battelle porous materials, and commercial porous materials such as GE Foametal, Huyck Feltmetal, and Pall Rigimesh, and porous metals. Various shapes and materials were made into chamber inserts and tested.

The IM-SPG is capable of operating with any gas. Hydrogen, helium, and nitrogen are normally used. For this test program, hydrogen was used for all tests. It offered low cost, greater dynamic amplitudes, and a higher frequency range than that obtainable with other gases.

Data and Accuracy

The primary performance data of the generator are the frequency, oscillation pressure amplitude, and average chamber pressure. For this test series, waveform spectral content was included. For each generator operating mode the oscillation pressure amplitude is a percentage of the average chamber pressure at each frequency. This function is essentially independent of average chamber pressure magnitude. Thus, the ratio of peak-to-peak pressure amplitude to average chamber pressure may be plotted as a function of frequency for each mode. This is the form used for reporting the data in the next section. The actual peak-to-peak pressure amplitude at any desired frequency is found by multiplying the above ratio by the corresponding average chamber pressure.

Estimated accuracy of the frequency measurement is $\pm$ 1 Hz. The cycle-to-cycle variation in oscillation pressure amplitude of the reference transducer output signal was found to be $\pm$ 2 percent in the worst cases. These variations are within the inaccuracies of reading the oscilloscope photographs,

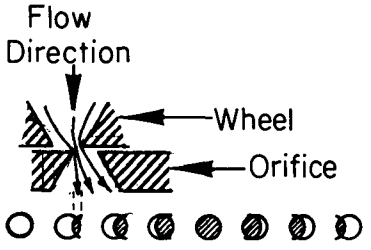

A. Cyclic Inlet Area Variaton Caused by Wheel Hole Passing Inlet Orifice and Showing Resultant Asymmetric Flow

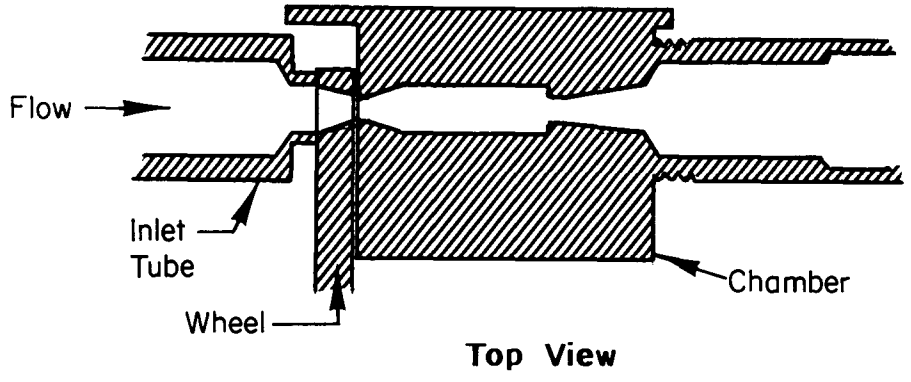

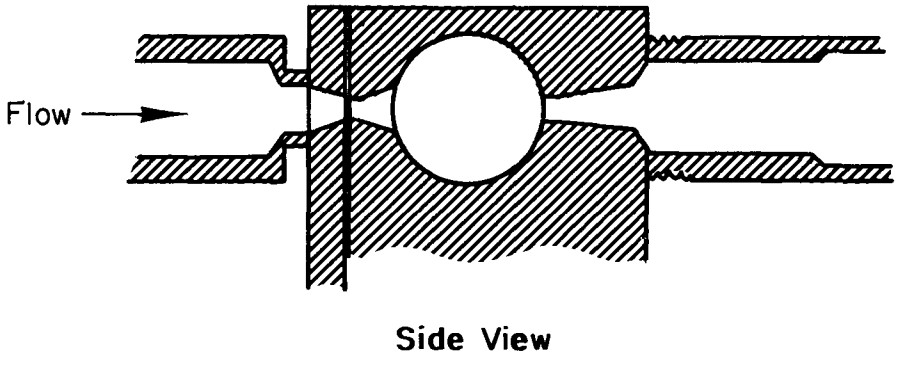

B. Overall IM-SPG Flow Geometry

FIGURE 4. IM-SPG FLOW GEOMETRY

which include low-frequency electronic noise (60 cycle) and waveform distortion. Average chamber pressure accuracy was $\pm$ 1/2 percent. The test-to-test variation or repeatibility of oscillation pressure amplitude each time a test condition was repeated was found to be normally $\pm$ 2 percent, and to reach $\pm$ 5 percent in a few worst cases.

Spectrum-analyzer data are given in the form of the ratio of the root-mean-square harmonic frequency amplitudes to the root-mean-square fundamental frequency amplitude. Filter and charge amplifier corrections at each appropriate frequency were applied to the amplitude data. Accuracy of the corrected spectrum-analyzer data is estimated at $\pm$ 3 percent.

RESULTS AND DISCUSSION

Chamber-Filler Development

A large number of porous-material samples were fabricated to fit into the IM-SPG chamber. These included several different grades (meshes) of screen or wire cloth, three grades (fine, medium coarse, and extra coarse) of steel wool, one of porous graphite, one of graphite cloth, five of GE Foametal, four of Michigan Dynamic Dynapore wire mesh laminates, three different grades (densities) of Huyck Feltmetal fiber metal materials, and twenty samples of Pall Rigimesh and PSS (sintered stainless steel powder).

Tests were performed first on a series of thin [up to 1/8-inch (0.32 cm) thick] specimens consisting of wire screen, wire mesh or laminate, and sintered metal powders. The specimens were placed against the flat 3/4-inch (1.92 cm)-diameter sides with nothing between. Large amplitude reductions of the high-frequency components were obtained along with minor reduction of the chamber harmonics. The best performance given by the flat liner specimens was with Pall Supramesh. This material is a 0.009-inch (0.032 cm)-thick material of SS304 powder on SS304 wire mesh. Two (finest and coarsest) of the steel-wool specimens were tried next. They reduced the harmonic amplitudes somewhat but they deteriorated rapidly. The specimen deterioration was gross crushing of the specimen, a cored hole from the inlet nozzle flow, and extrusion of material into and sometimes out of the outlet nozzle.

The graphite felt cloth completely collapsed against the outlet side of the chamber. The porous graphite specimen completely disintegrated and was blown out of the chamber. Next Pall Supramesh thin specimens were placed against the chamber flat ends as previously described and a center piece made of a screen-type wire spiral filled with fine steel wool was tried. This combination produced very good results. Both the harmonic and high-frequency components were significantly reduced. However, the specimen deteriorated rather quickly. After several test series, the inlet nozzle side of the specimen was crushed nearly mideway into the chamber and the exit nozzle side was pushed into the outlet nozzle. As a result of the deformation the waveform changed (harmonic component amplitudes increased) and chamber pressure increased.

Several other variations of the center specimen were tried. These involved different combinations of stronger wire screen for rigidity and fine mesh screen to hold the steel wool in place. Again the deterioration was unacceptable.

Finally, a series of specimens were tested involving various porous and woven-wire materials by themselves completely filling the chamber and then in combination with the Pall Supramesh end pieces. The best results (low-harmonic- and high-frequency-component amplitude reduction with negligible deterioration) were obtained using a two-material, three-piece, chamber insert. One piece of Pall Supramesh was placed essentially against each of the flat ends of the chamber--these are the chamber ends through which the reference and test transducers are flush mounted. A 0.007-inch (0.018 cm)-thick spacer was placed between the flush-mounted pressure transducers and Pall Supramesh end pieces to prevent interference between the transducer diaphram and Supramesh. Between these two end pieces a 20 percent dense Feltmetal piece was used to fill the rest of the chamber. A photograph of the IM-SPG chamber and the three-piece filter insert is shown in Figure 5.

A complete series of performance tests of the IM-SPG with this three-piece, two material chamber insert were made. The results of these perfromance tests are given in the following section.

IM-SPG Performance

Tests were made at low [30-50 psia (21-35 N/cm^2abs)]and high [150-300 psia (104-207 N/cm^2abs)] pressure levels at frequencies of 100, 1,000, 3,000, 5,000, and 10,000 Hz. These tests correspond to those called for in the original program plan. Several additional tests were performed at other pressure levels and frequencies. This complete test series was performed using the IM-SPG with one inlet and one outlet.

Tests were also made with the IM-SPG in two other modes using the two additional static-pressure nozzles. These extra nozzles allow independent control of oscillation pressure amplitude and static or bias pressure. Tests were performed first with the two additional nozzles acting as flow inlets (minimum amplitude), then acting as flow outlets (maximum amplitude). Thus, these tests represent the extremes of the IM-SPG performance envelope.

Typical waveforms over the range of frequencies and pressures are shown in Figures 6 through 9. Both filtered (50-kHz low pass) and unfiltered signals are shown. In all dual-waveform figures the upper waveform has been filtered and the lower waveform is the corresponding unfiltered one. Also shown are the typical corresponding spectral contents measured by the spectrum analyzer. The phase difference between the filtered and unfiltered pressure waveform is due to a phase shift by the filter and to the small difference in oscilloscope external-trigger sensitivities on the two oscilloscope time-base units used.

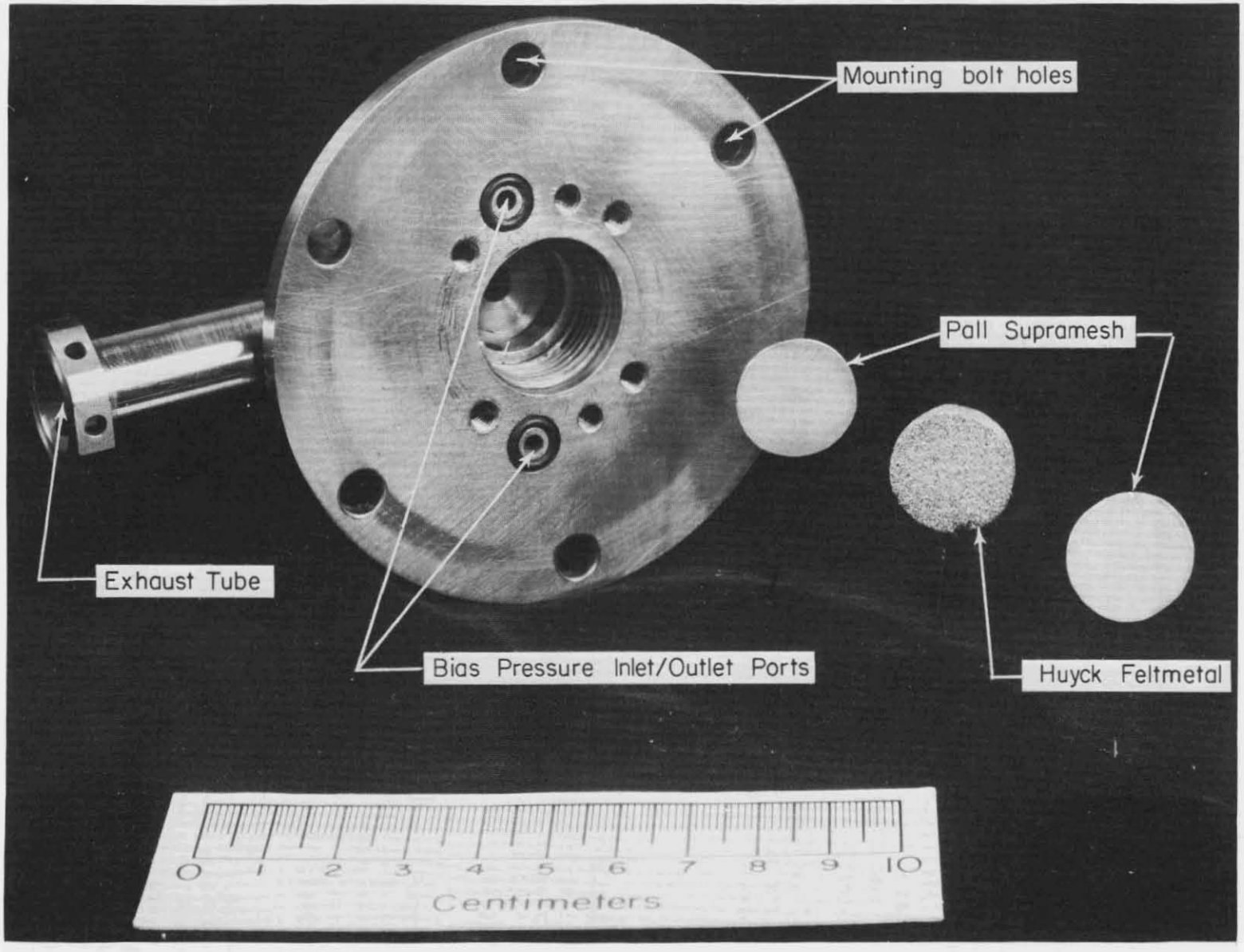

FIGURE 5. IM-SPG CHAMBER AND ACOUSTIC ABSORBING FILLER PIECES

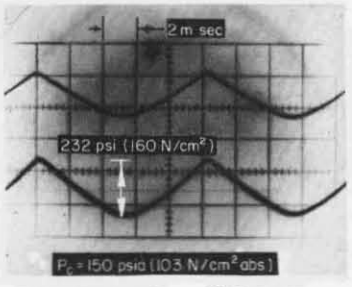

a. Waveform at 100 Hz

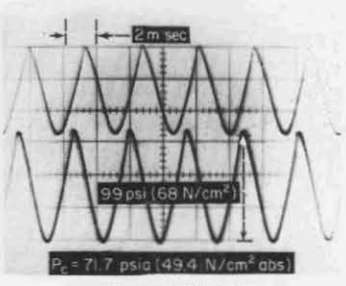

c. Waveform at 300 Hz

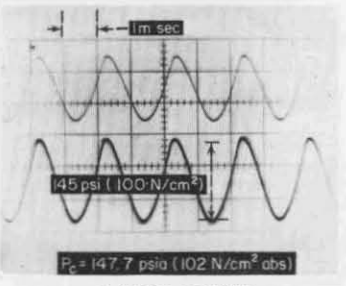

e. Waveform at 500 Hz

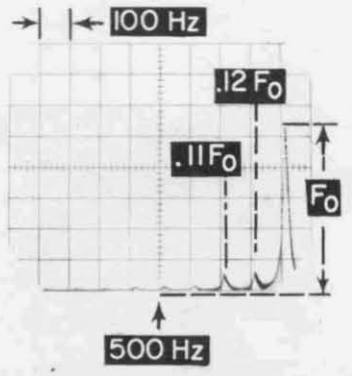

b. Unfiltered Waveform Frequency Spectrum; Fundamental Frequency, 100 Hz

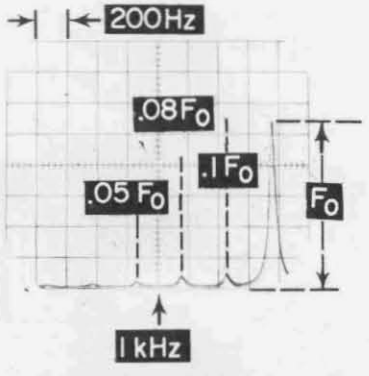

d. Unfiltered Waveform Frequency Spectrum; Fundamental Frequency, 300 Hz

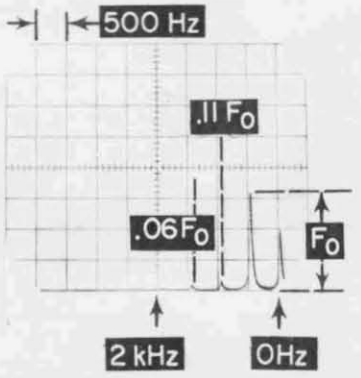

f. Unfiltered Waveform Frequency Spectrum; Fundamental Frequency, 500 Hz

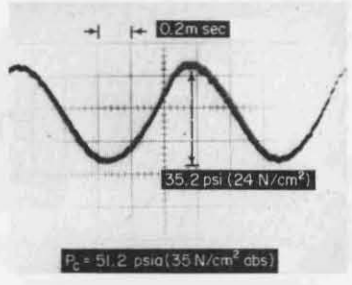

g. Unfiltered Waveform at 1 kHz

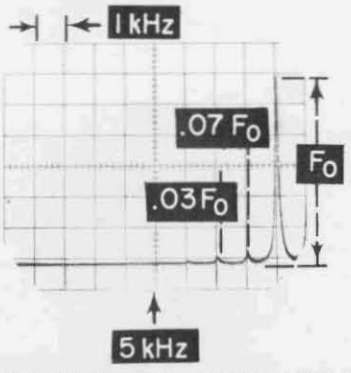

h. Unfiltered Waveform Frequency Spectrum; Fundamental Frequency, 1 kHz

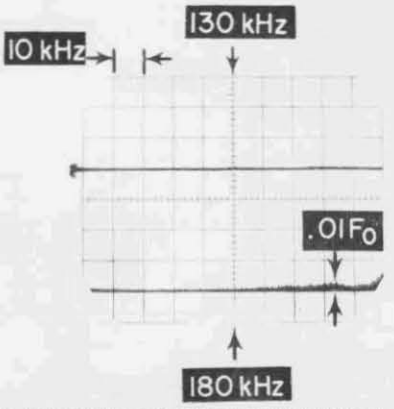

i. Unfiltered Waveform Frequency Spectrum; Fundamental Frequency, 1 kHz

Figure 6. Pressure waveforms and frequency spectrums at low frequencies from oscilloscope. Lower waveform is unfiltered and upper waveform is the same signal after 50 kHz low-pass filtering. IM-SPG with one inlet and one outlet.

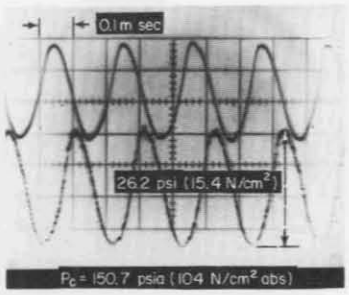

a. Waveform at 5 kHz

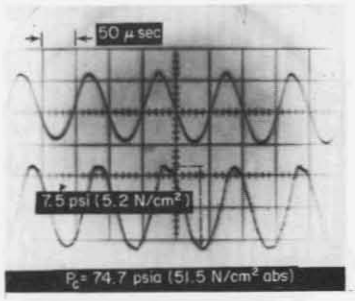

c. Waveform at 10 kHz

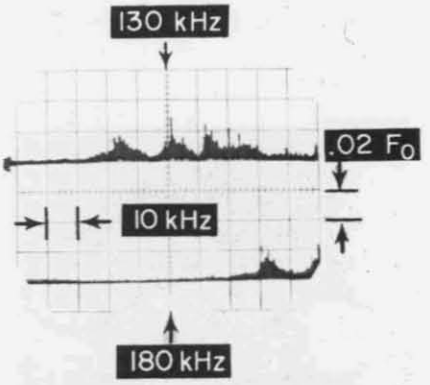

e. Unfiltered Waveform Frequency Spectrum; Fundamental Frequency, 10 kHz

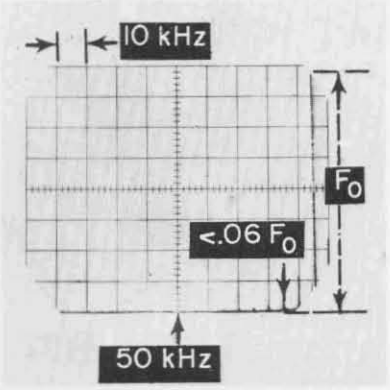

b. Unfiltered Waveform Frequency Spectrum; Fundamental Frequency, 5 kHz

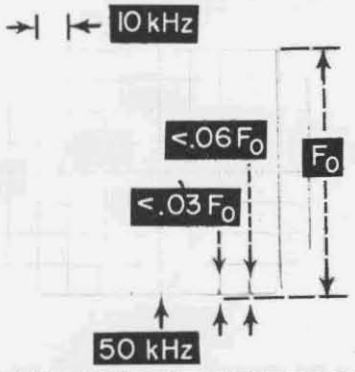

d. Unfiltered Waveform Frequency Spectrum; Fundamental Frequency, 10 kHz

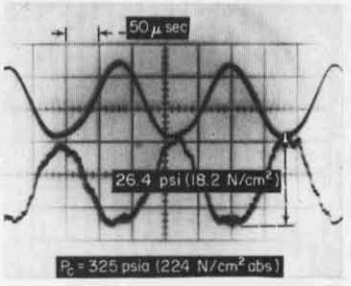

f. Waveform at 15 kHz

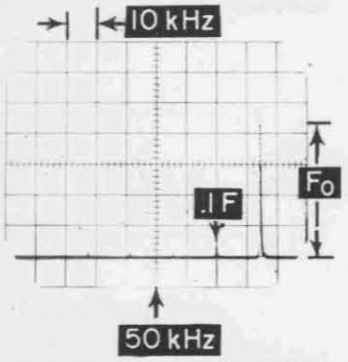

g. Unfiltered Waveform Frequency Spectrum; Fundamental Frequency, 15 kHz

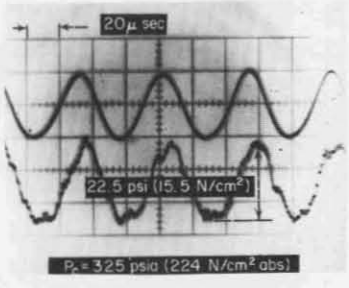

h. Waveform at 20 kHz

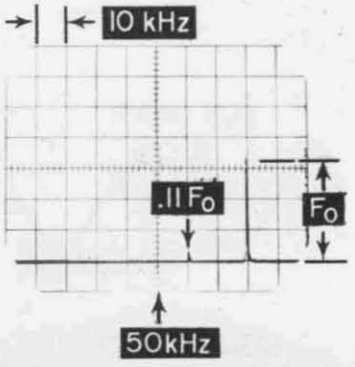

i. 50 kHz Low-Pass Filtered Waveform Frequency Spectrum; Fundamental Frequency, 20 kHz

Figure 7. Pressure waveforms and frequency spectrums at high frequencies from oscilloscope. IM-SPG with one inlet and one outlet.

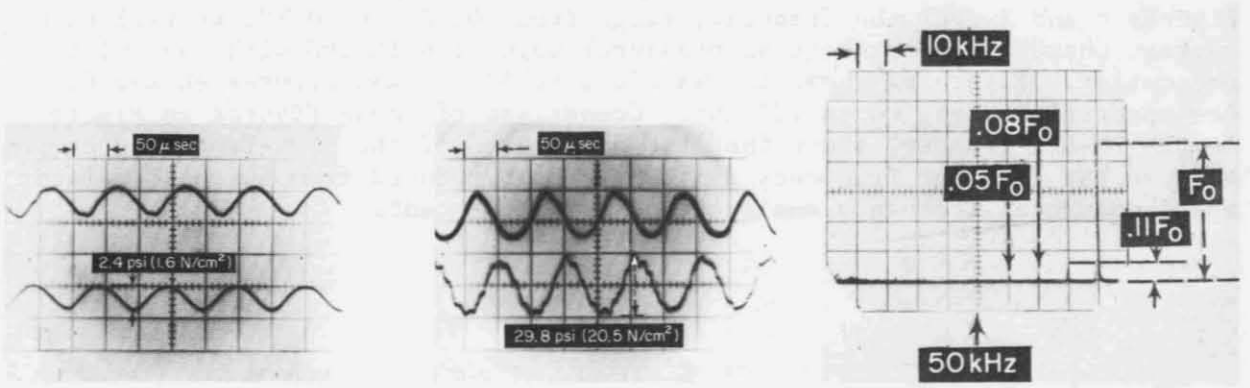

a. Waveform at 30 psia (20 N/cm² abs) Bias Pressure

b. Waveform at 315 psia (217 N/cm² abs) Bias Pressure

c. Unfiltered Waveform Frequency Spectrum; Fundamental Frequency, 10 kz

Figure 8. Pressure waveform and frequency spectrum at two bias pressures at 10 kHz fundamental frequency. 1M-SPG with one inlet and one outlet.

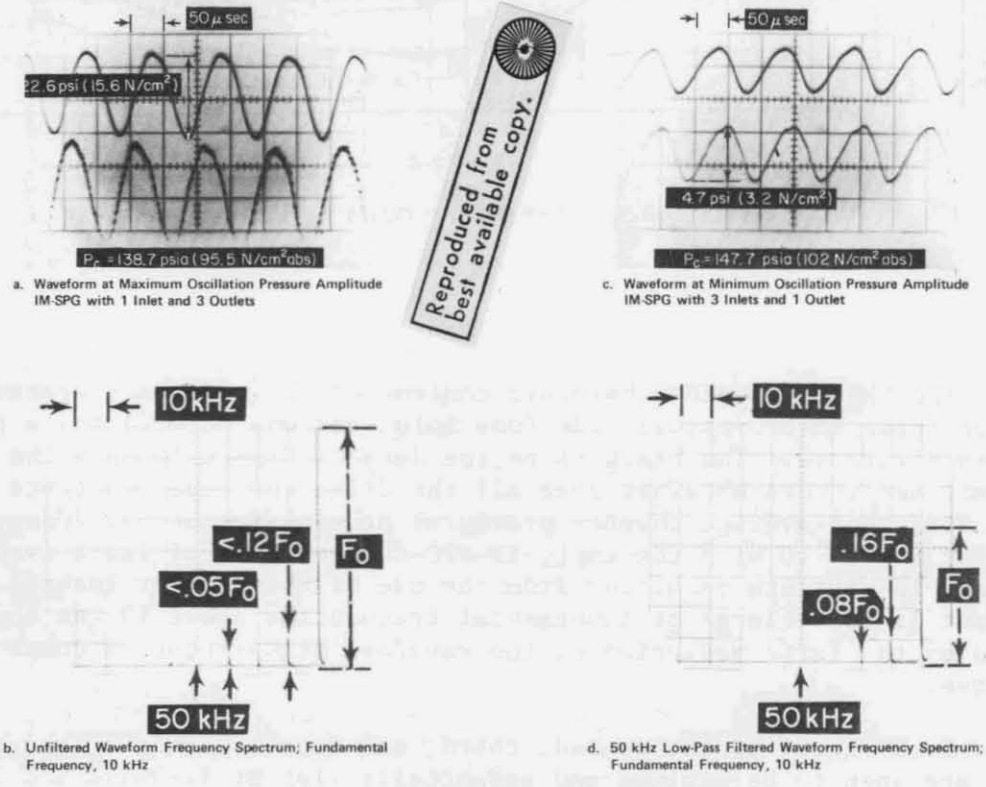

a. Waveform at Maximum Oscillation Pressure Amplitude IM-SPG with 1 Inlet and 3 Outlets

c. Waveform at Minimum Oscillation Pressure Amplitude IM-SPG with 3 Inlets and 1 Outlet

b. Unfiltered Waveform Frequency Spectrum; Fundamental Frequency, 10 kHz

d. 50 kHz Low-Pass Filtered Waveform Frequency Spectrum; Fundamental Frequency, 10 kHz

Figure 9. Pressure waveform and frequency spectrum at maximum and minimum oscillation pressure amplitude at 10 kHz fundamental frequency.

Waveforms and their associated frequency spectrums are shown in Figures 6 and 7 over the frequency range from 100 Hz to 20 kHz at various high average chamber pressures (bias pressure) using the IM-SPG with one inlet and one outlet. Figure 6g shows the waveform at 10 kHz and Figures 6h and 6i show its spectral content up to 230 kHz. Comparison of these Figures to Figure 3 (empty IM-SPG chamber) shows that the amplitudes of the high-frequency components in the resonant frequency range have been reduced from 60 to 80 percent of the fundamental frequency amplitude to 2 to 3 percent.

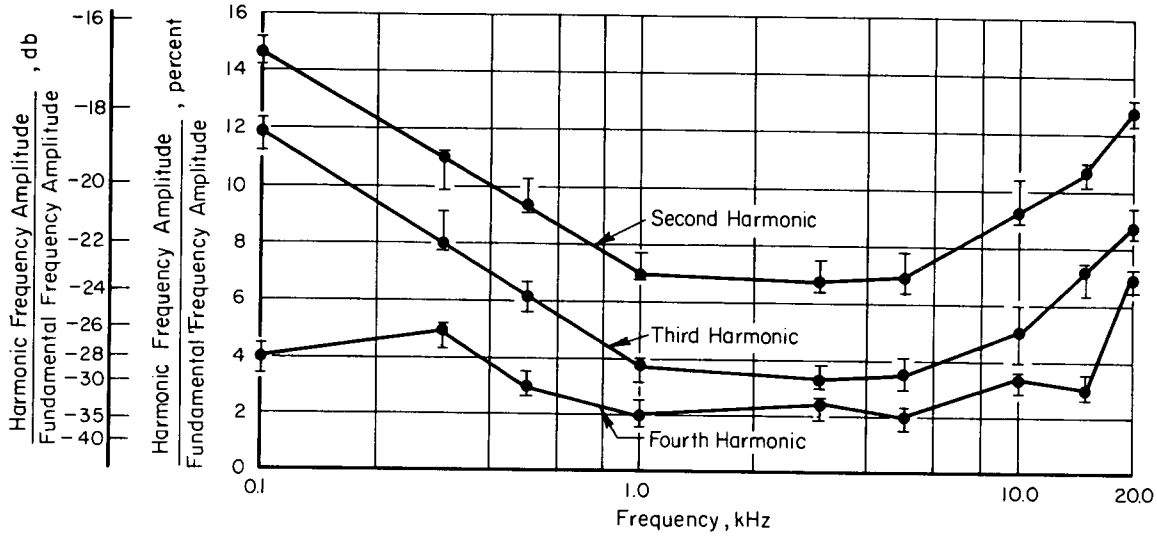

FIGURE 10. IM-SPG REFERENCE TRANSDUCER OUTPUT WAVEFORM HARMONIC CONTENT

The IM-SPG waveform harmonic content of the reference transducer's output for these IM-SPG normal-mode (one inlet and one outlet) tests are summarized in Figure 10. The brackets on the data of Figure 10 show the spread of harmonic amplitudes obtained over all the different repeated tests and the tests at different average chamber pressures at each frequency. Comparison of the data of Figure 10 with the empty-IM-SPG-chamber data of Table 1 shows the improvement in waveform resulting from the use of the chamber inserts. This improvement is quite large at fundamental frequencies above 10 kHz and is accompanied by the large reduction of the waveform high-frequency components noted above.

From Figure 10 the second, third, and fourth harmonic frequency amplitudes are seen to be minimum and essentially flat at 7, 3-1/2 and 2 percent of the fundamental frequency amplitude in the frequency range of normal interests, 1 to 5 kHz. These harmonic components increase at both lower and higher frequencies. The increase at lower frequencies is attributed to lessening of the inlet flow smoothing effects. From Figures 6a through 6f it is seen that

the pressure waveform approaches the actual area-variation waveform caused by a circular hole passing a circular hole. The resulting waveform is not sinusoidal.[4] The increase in amplitude of the higher harmonics at the higher frequencies (see also Figures 7f-7i) is attributed to the driving frequency approaching the chamber resonance frequency and the next-higher chamber response mode (second tangential mode).

The effect of different bias pressures on waveform for one frequency is shown in Figure 8 with the IM-SPG in its normal mode. The waveform at 10 kHz at a bias pressure of 29 psia (20 N/cm^2abs) is given in Figure 8a. The waveform and its harmonic spectrum for the same fundamental frequency at 325 psia (224 N/cm^2abs) is given in Figures 8b and 8c. Figures 7c and 7d are for a third bias pressure, 74.7 psia (51.5 N/cm^2abs) at this frequency. There is seen to be little effect of bias pressure on the waveform harmonic amplitudes. It was noted that increasing bias pressure did increase the resonant frequency-range amplitudes by several percent over the bias pressure range covered.

Waveforms at three different oscillation pressure amplitudes (three different IM-SPG modes) at one frequency are given in Figures 7c, 7d, and 9. Similar waveforms (and harmonic content) to those for the IM-SPG normal mode were found for the maximum oscillation pressure amplitude mode (one modulated inlet, three outlets). Poorer waveforms were obtained with the generator in the minimum oscillator pressure amplitude mode (three inlets, one outlet). The poorer waveform was more prevalent at low frequencies where oscillation pressure amplitudes are large. Second- and third-harmonic-frequency amplitudes up to 1/3 of the fundamental-frequency amplitude were found at low frequencies (1 kHz and below). This high harmonic content at low frequencies is attributed to the fact that the inlet nozzles were not choked throughout most of a cycle. The porous filler-chamber inserts reduced the pressure ratio across the inlet nozzle by increasing the average chamber pressure. The chamber pressure increase is attributed to the effective flow area of the chamber inserts being smaller than the exit nozzle area which controls the pressure.

The peak-to-peak oscillation pressure amplitude from all of the tests are shown in Figure 11. Also shown is the corresponding IM-SPG performance with an empty chamber (no acoustic filler) taken from Reference 2. The reduction of oscillation pressure amplitude is roughly a factor of two. The general trends of the performance of the two chamber conditions are seen to be quite similar. Even with the decreased amplitude caused by the chamber acoustic filler, 15 percent of bias pressure peak-to-peak oscillation pressure amplitude was obtained at 10 kHz. Thus, for an average chamber pressure of 300 psia (207 N/cm^2abs), the peak-to-peak oscillation-pressure-fundamental amplitude is 45 psi (31 N/cm^2). The waveform has a second harmonic-frequency amplitude of 9 percent [2 psi (1.8 N/cm^2)], a third harmonic-frequency amplitude of 5 percent [1.1 psi (0.9 N/cm^2)], and a fourth harmonic-frequency amplitude of 3 percent [0.6 psi (0.4 N/cm^2)] of the fundamental frequency amplitude. The acoustic energy in all of these harmonics is about 1 percent of the energy in the fundamental.

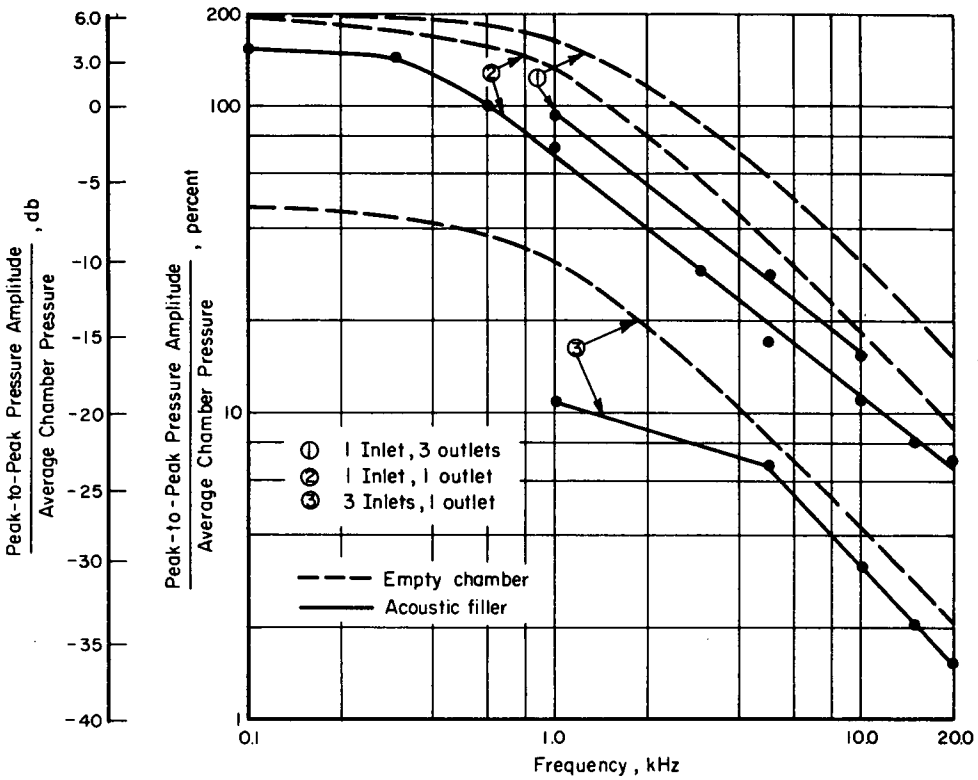

FIGURE 11. PEAK-TO-PEAK SINUSOIDAL PRESSURE AMPLITUDE AS A PERCENT OF AVERAGE CHAMBER PRESSURE AS A FUNCTION OF FREQUENCY USING HYDROGEN AS THE TEST GAS

SUMMARY OF RESULTS

The waveform of the IM-SPG was significantly improved at any particular oscillation-pressure amplitude and bias-pressure ratio, especially at high frequencies. Harmonic content was significantly reduced at all frequencies (up to a factor of over five at 10 kHz). Also the previous excessive high-frequency transducer resonant-frequency amplitudes of up to 60 to 80 percent of the fundamental frequency amplitude were essentially eliminated (reduced to 2-3 percent maximum). However, these gains were accompanied by a reduction in available oscillation pressure amplitude by approximately a factor of two. The waveform improvement was achieved by using a special three-piece, two-material chamber insert. The useable range of the sinusoidal pressure generator has been extended from several kilohertz to 10 to 20 kilohertz depending on the desired accuracy requirements. The need for an electronic filter on the transducer output signal has essentially been eliminated.

CONCLUDING REMARKS

While significant improvement in the IM-SPG performance has been obtained, extensive efforts to obtain optimum performance were not made. Additional improvement in both waveform quality and an increase in oscillation-pressure amplitude should be possible with further development. Part of that development should be directed toward detailed determination of average and oscillation pressure throughout the chamber to ensure chamber pressure uniformity.

APPENDIX

CORRECTIONS TO DATA

The reference pressure transducer's output signal was conditioned by a charge amplifier and then filtered. The charge amplifier was used at all times. The charge amplifiers were calibrated for dynamic response in accordance with the manufacturers instructions. The transducer data were corrected using the dynamic response characteristics so determined and are given in Figures A-1 and A-2. Similar calibration and corrections were performed for the high-frequency dual-channel filter. These data are given in Figure A-3.

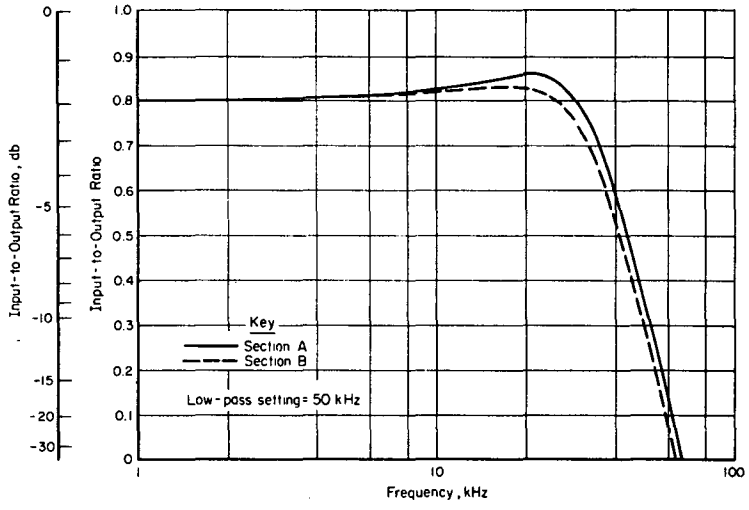

FIGURE A-1. DUAL CHANNEL FILTER SECTION LOW-PASS RESPONSE CHARACTERISTICS

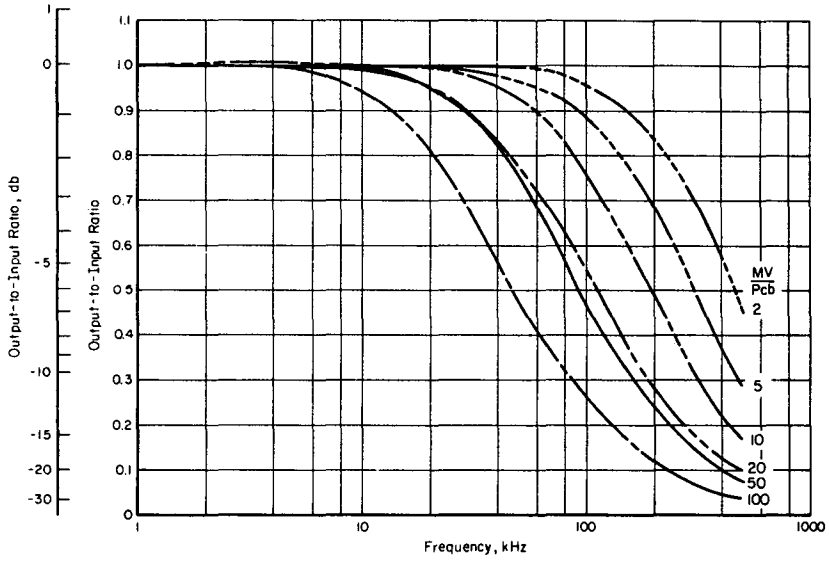

FIGURE A-2. REFERENCE TRANSDUCER CHARGE AMPLIFIER FREQUENCY RESPONSE CHARACTERISTICS

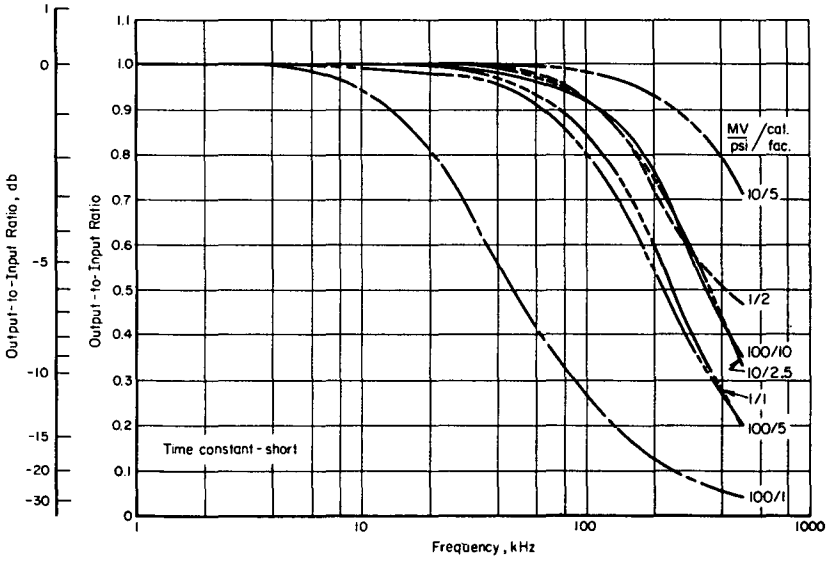

FIGURE A-3. TEST TRANSDUCER CHARGE AMPLIFIER FREQUENCY RESPONSE CHARACTERISTICS

REFERENCES

(1) Robinson, R. E., and Liu, C. Y., "Resonant Systems for Dynamic Transducer Evaluations", NASA CR-72435 (August 31, 1968).

(2) Robinson, R. E., "Development of a Sinusoidal Pressure Generator for Pressure Transducer Dynamic Calibration", NASA CR-72656 (March 25, 1970).

(3) Robinson, R. E., "Dynamic Response of High-Frequency Pressure Transducers to Large Amplitude Sinusoidal Pressure Oscillations", NASA CR-2000 (In publication).

(4) Bentley, W. C., and Walter, J. J., "Dynamic Response Testing of Transient Pressure Transducers for Liquid Propellant Rocket Combustion Chambers", Aeronautical Engineering Report No. 595g, Princeton University (May, 1963).

DISTRIBUTION LIST

Dr. R. J. Priem MS 500-209 (2)
NASA Lewis Research Center
21000 Brookpark Road
Cleveland, Ohio 44135

Norman T. Musial
NASA Lewis Research Center
21000 Brookpark Road
Cleveland, Ohio 44135

Library (2)
NASA Lewis Research Center
21000 Brookpark Road
Cleveland, Ohio 44135

Report Control Office
NASA Lewis Research Center
21000 Brookpark Road
Cleveland, Ohio 44135

Brooklyn Polytechnic Institute
Attn: V. D. Agosta
Long Island Graduate Center
Route 110
Farmingdale, New York 11735

Chemical Propulsion Information Agency
John Hopkins University/APL
Attn: T. W. Christian
8621 Georgia Avenue
Silver Spring, Maryland 20910

NASA
Lewis Research Center
Attn: E. W. Conrad, MS 500-204
21000 Brookpark Road
Cleveland, Ohio 44135

North American Rockwell Corporation
Rocketdyne Division
Attn: L. P. Combs, D/991-350 Zone 11
6633 Canoga Avenue
Canoga Park, California 91304

Aerospace Corporation
Attn: O. W. Dykema
Post Office Box 95085
Los Angeles, California 90045

Ohio State University
Department of Aeronautical and Astronautical Engineering
Attn: R. Edse
Columbus, Ohio 43210

TRW Systems
Attn: G. W. Elverum
One Space Park
Redondo Beach, California 90278

Bell Aerospace Company
Attn: T. F. Ferger
Post Office Box 1
Mail Zone J-81
Buffalo, New York 14205

Pratt & Whitney Aircraft
Florida Research & Development Center
Attn: G. D. Garrison
Post Office Box 710
West Palm Beach, Florida 33402

NASA
Lewis Research Center
Attn: L. Gordon, MS 500-209
21000 Brookpark Road
Cleveland, Ohio 44135

Purdue University
School of Mechanical Engineering
Attn: R. Goulard
Lafayette, Indiana 47907

Air Force Office of Scientific Research
Chief Propulsion Division
Attn: Lt. Col. R. W. Haffner (NAE)
1400 Wilson Boulevard
Arlington, Virginia 22209

National Technical Information (40)
Service
Springfield, Virginia 22151

NASA Representative (2)
NASA Scientific and Technical
Information Facility
P. O. Box 33
College Park, Maryland 20740
(2 Copies with Document Release
Authorization Form)

University of Illinois
Aeronautics/Astronautic Engineering
Department
Attn: R. A. Strehlow
Transportation Building, Room 101
Urbana, Illinois 61801

NASA
Manned Spacecraft Center
Attn: J. G. Thibadaux
Houston, Texas 77058

Massachusetts Institute of Technology
Department of Mechanical Engineering
Attn: T. Y. Toong
77 Massachusetts Avenue
Cambridge, Massachusetts

Illinois Institute of Technology
Attn: T. P. Torda
Room 200 M. H.
3300 S. Federal Street
Chicago, Illinois 60616

AFRPL
Attn: R. R. Weiss
Edwards, California 93523

U. S. Army Missile Command
AMSMI-RKL, Attn: W. W. Wharton
Redstone Arsenal, Alabama 35808

University of California
Aerospace Engineering Department
Attn: F. A. Williams
Post Office Box 109
LaJolla, California 92037

Pennsylvania State University
Mechanical Engineering Department
Attn: F. M. Faeth
207 Mechanical Engineering Department
University Park, Pennsylvania 16802

TISIA
Defense Documentation Center
Cameron Station
Building 5
5010 Duke Street
Alexandria, Virginia 22314

Office of Assistant Director
(Chemical Technician)
Office of the Director of Defense
Research and Engineering
Washington, D.C. 20301

D. E. Mock
Advanced Research Projects Agency
Washington, D.C. 20525

Dr. H. K. Doetsch
Arnold Engineering Development Center
Air Force Systems Command
Tullahoma, Tennessee 37389

Library
Air Force Rockept Propulsion Laboratory
(RPR)
Edwards, California 93523

Library
Bureau of Naval Weapons
Department of the Navy
Washington, D. C.

Library
Director (Code 6180)
U. S. Naval Research Laboratory
Washington, D.C. 20390

APRP (Library)
Air Force Aero Propulsion Laboratory
Research and Technology Division
Air Force Systems Command
United States Air Force
Wright-Patterson AFB, Ohio 45433

Georgia Institute of Technology
Aerospace School
Attn: B. T. Zinn
Atlanta, Georgia 30332

Marshall Industries
Dynamic Science Division
2400 Michelson Drive
Irvine, California 92664

Mr. Donald H. Dahlene
U. S. Army Missile Command
Research, Development, Engineering
and Missile Systems Laboratory
Attn: AMSMI-RK
Redstone Arsenal, Alabama 35809

Princeton University
James Forrestal Campus Library
Attn: D. Harrje
Post Office Box 710
Princeton, New Jersey 08540

U. S. Naval Weapons Center
Attn: T. Inouye, Code 4581
China Lake, California 93555

Office of Naval Research
Navy Department
Attn: R. D. Jackel, 473
Washington, D.C. 20360

Air Force Aero Propulsion Laboratory
Attn: APTC Lt. M. Johnson
Wright-Patterson AFB, Ohio 45433

Naval Underwater Systems Center
Energy Conversion Department
Attn: Dr. R. S. Lazar, Code TB 131
Newport, Rhode Island 02840

NASA
Langley Research Center
Attn: R.S. Levine, MS 213
Hampton, Virginia 23365

Aerojet General Corporation
Attn: David A. Fairchild,
Mech. Design
Post Office Box 15847 (Sect. 9732)
Sacramento, California 95809

Technical Information Department
Aeronutronic Division of Philco Ford
Corporation
Ford Road
Newport Beach, California 92663

Library-Documents
Aerospace Corporation
2400 E. El Segundo Boulevard
Los Angeles, California 90045

University of Michigan
Aerospace Engineering
Attn: J. A. Nicholls
Ann Arbor, Michigan 48104

Tulane University
Attn: J. C. O'Hara
6823 St. Charles Avenue
New Orleans, Louisiana 70118

University of California
Department of Chemical Engineering
Attn: A. K. Oppenheim
6161 Etcheverry Hall
Berkeley, California 94720

Army Ballistics Laboratories
Attn: J. R. Osborn
Aberdeen Proving Ground, Maryland 21005

Sacramento State College
School of Engineering
Attn: F. H. Reardon
6000 J. Street
Sacramento, California 95819

Purdue University
School of Mechanical Engineering
Attn: B. A. Reese
Lafayette, Indiana 47907

NASA
George C. Marshall Space Flight Center
Attn: R. J. Richmond, SNE-ASTN-PP
Huntsville, Alabama 35812

Colorado State University
Mechanical Engineering Department
Attn: C. E. Mitchell
Fort Collins, Colorado 80521

University of Wisconsin
Mechanical Engineering Department
Attn: P. S. Myers
1513 University Avenue
Madison, Wisconsin 53706

North American Rockwell Corporation
Rocketdyne Division
Attn: J. A. Nestlerode,
AC46 D/596-121
6633 Canoga Avenue
Canoga Park, California 91304

Library
Bell Aerosystems, Inc.
Box 1
Buffalo, New York 14205

Report Library, Room 6A
Battelle Memorial Institute
505 King Avenue
Columbus, Ohio 43201

D. Suichu
General Electric Company
Flight Propulsion Laboratory
Department
Cincinnati, Ohio 45215

Library
Ling-Temco-Vought Corporation
Post Office Box 5907
Dallas, Texas 75222

Marquardt Corporation
16555 Saticoy Street
Box 2013 - South Annex
Van Nuys, California 91409

P. F. Winternitz
New York University
University Heights
New York, New York

Jet Propulsion Laboratory
California Institute of Technology
Attn: J. H. Rupe
4800 Oak Grove Drive
Pasadena, California 91103

University of California
Mechanical Engineering Thermal Systems
Attn: Prof. R. Sawyer
Berkeley, California 94720

ARL (ARC)
Attn: K. Scheller
Wright-Patterson AFB, Ohio 45433

Library
Susquehanna Corporation
Atlantic Research Division
Shirley Highway and Edsall Road
Alexandria, Virginia 22314

STL Tech. Lib. Doc. Acquisitions
TRW System Group
One Space Park
Redondo Beach, California 90278

Dr. David Altman
United Aircract Corporation
United Technology Center
Post Office Box 358
Sunnyvale, California 94088

Library
United Aircraft Corporation
Pratt and Whitney Division
Florida Research and Development Center
Post Office Box 2691
West Palm Beach, Florida 33402

Library
Air Force Rocket Propulsion Laboratory
(RPM)
Edwards, California 93523

Allan Hribar, Assistant Professor
Post Office Box 5014
Tennessee Technological University
Cookeville, Tennessee 38501

I. Forsten
Picatinny Arsenal
Dover, New Jersey 07801

R. Stiff
Propulsion Division
Aerojet-General Corporation
Post Office Box 15847
Sacramento, California 95803

Library, Department 596-306
Rocketdyne Division of Rockwell
North American Rockwell Inc.
6633 Canoga Avenue
Canoga Park, California 91304

Library
Stanford Research Institute
333 Ravenswood Avenue
Menlo Park, California 94025

NASA
Lewis Research Center
Attn: E. O. Bourke MS 500-209
21000 Brookpark Road
Cleveland, Ohio 44135

NASA
Lewis Research Center
Attn: D. L. Nored 500-203
21000 Brookpark Road
Cleveland, Ohio 44135

NASA
Lewis Research Center MS 500-313
Rockets & Spacecraft Procurement Section
21000 Brookpark Road
Cleveland, Ohio 44135